Supporting information:

In-situ Bridging Nanotwinned All-solid-state Z-scheme g-C_3N_4/$CdCO_3$/CdS Heterojunction Photocatalyst by Metal Oxide for H_2 Evolution

Jing Wang, [a] *Yulei Fan,* [a] *Runhui Pan,* [a] *Qi Hao,* [a] *Jilei Ye,*[*a] *Yuping Wu,*[*a] *Teunis van Ree* [b]

[a] State Key Laboratory of Materials-oriented Chemical Engineering,

College of Chemical Engineering and School of Energy Science and Engineering, Nanjing Tech University, Nanjing, Jiangsu, 211816, China

[b] Department of Chemistry, University of Venda, Thohoyandou, 0950, South Africa

[*] *Corresponding authors: yejilei@njtech.edu.cn; wuyp@njtech.edu.cn (Wu)*

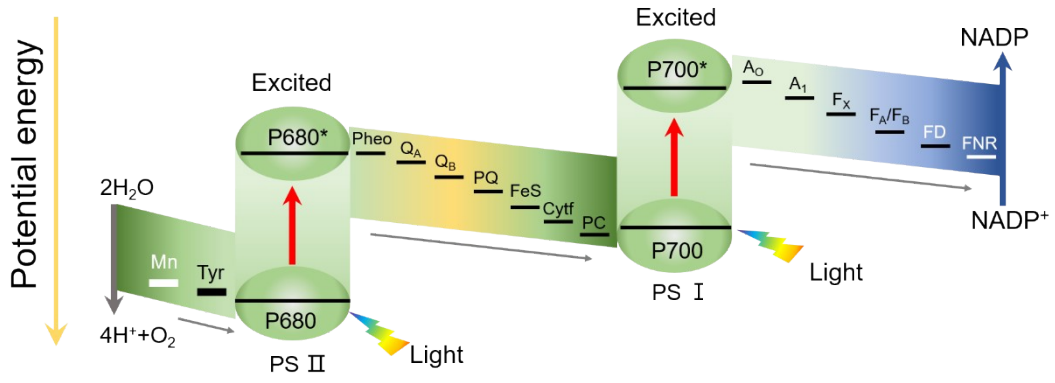

Fig. S1 Charge separation mechanism in natural photosynthesis [1, 2]. P680: pigment (chlorophyll) that absorbs 680 nm light in photosystem II (PSII); $P680^*$: the excited state of P680; P700: pigment (chlorophyll) that absorbs 700 nm light in photosystem I (PSI); $P700^*$: the excited state of P700. Mn: manganese calcium oxide cluster; Tyr: tyrosine in PSII; Pheo: pheophytin, the primary electron acceptor of PSII; Q_A: primary plastoquinone electron acceptor; Q_B: secondary plastoquinone electron acceptor; PQ: plastoquinone; FeS: Rieske iron sulphur protein; Cyt. f: cytochrome f; PC: plastocyanin; A_0: primary electron acceptor of PSI; A_1: phylloquinone; F_X, F_A, F_B: three separate iron sulphur centres; FD: ferredoxin; FNR: nicotinamide adenine dinucleotide phosphate (NADP) reductase.

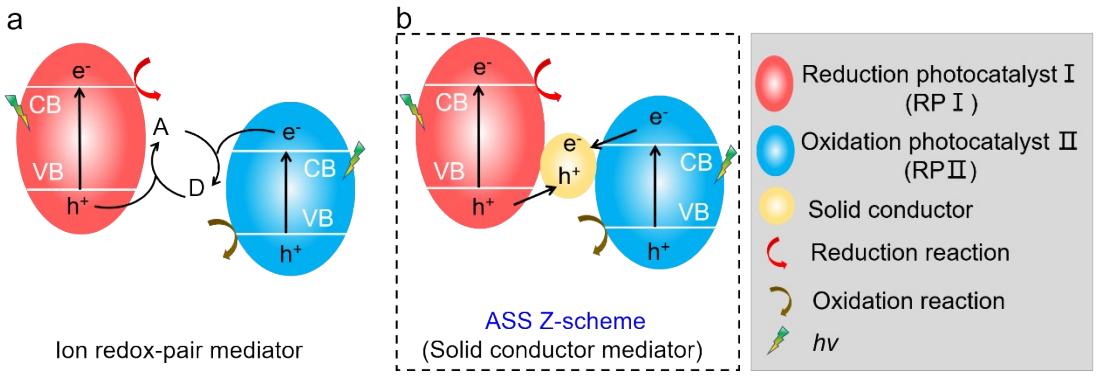

Fig. S2 Artificial Z-scheme photocatalysts. (a) Ion redox-pair mediator; (b) ASS Z-scheme system with solid conductor mediator.

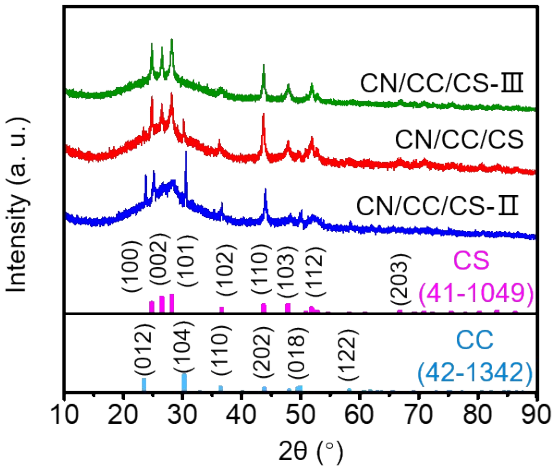

Fig. S3 XRD patterns of CN/CC/CS, CN/CC/CS-II, and CN/CC/CS-III.

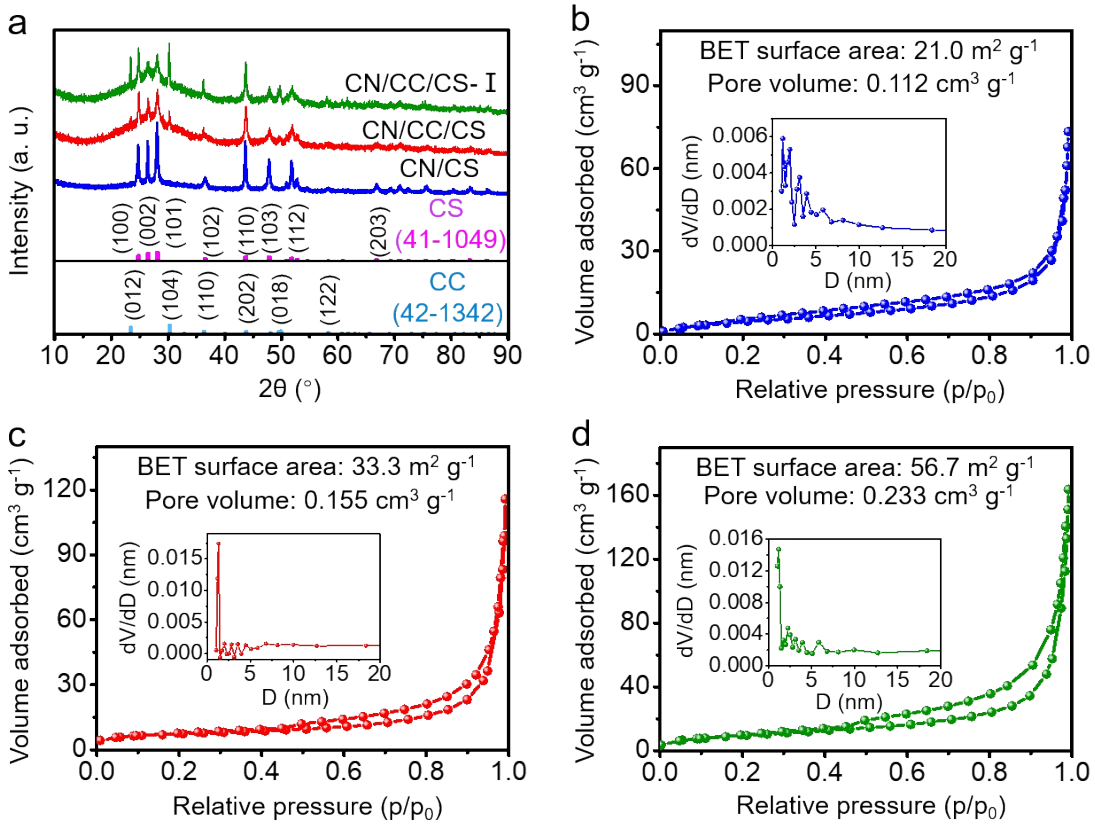

Fig. S4 (a) XRD patterns of CN/CS, CN/CC/CS, CN/CC/CS-I; (b-d) N_2 adsorption-desorption isotherms and pore size distribution plots of CN/CS, CN/CC/CS, and CN/CC/CS-I, respectively.

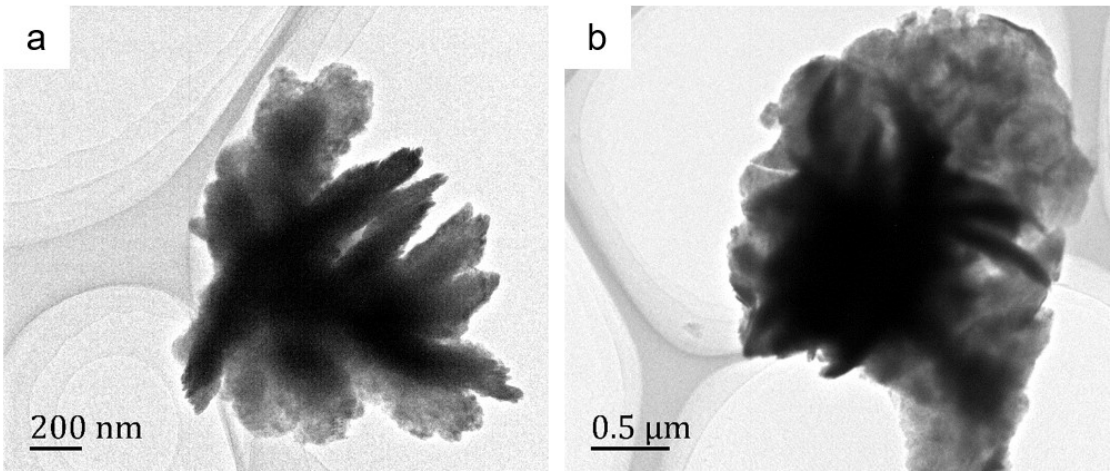

Fig. S5 Low-magnification TEM images of (a) CN/CS; (b) CN/CC/CS.

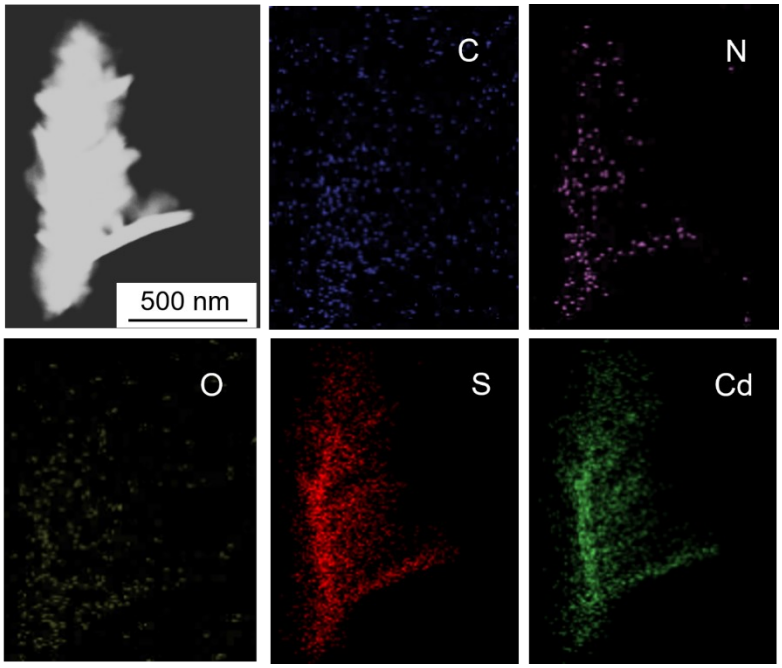

Fig. S6 The elemental mapping images of CN/CS.

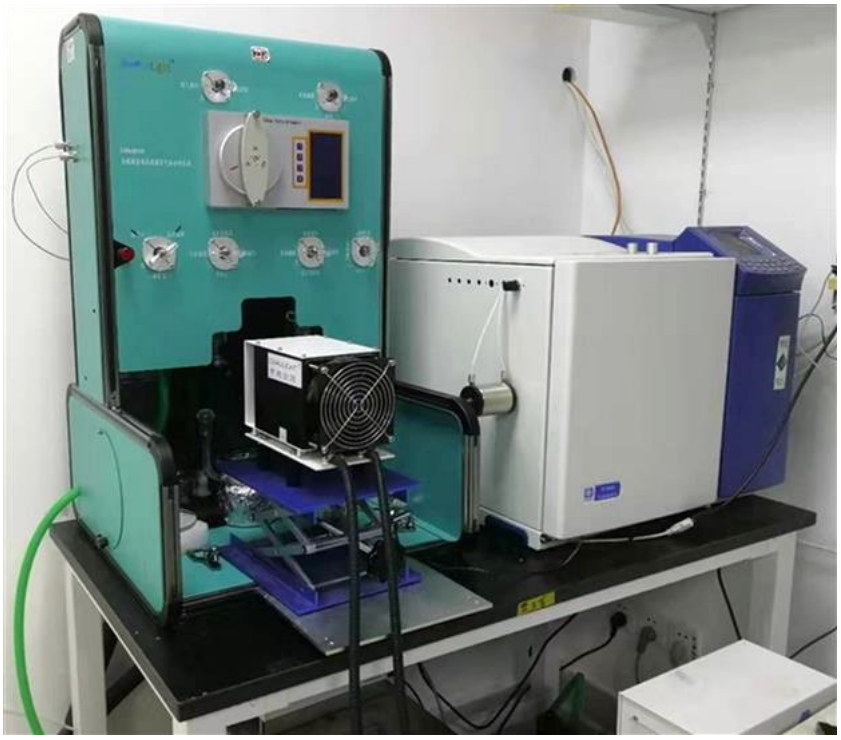

Fig. S7 Online photocatalytic test system.

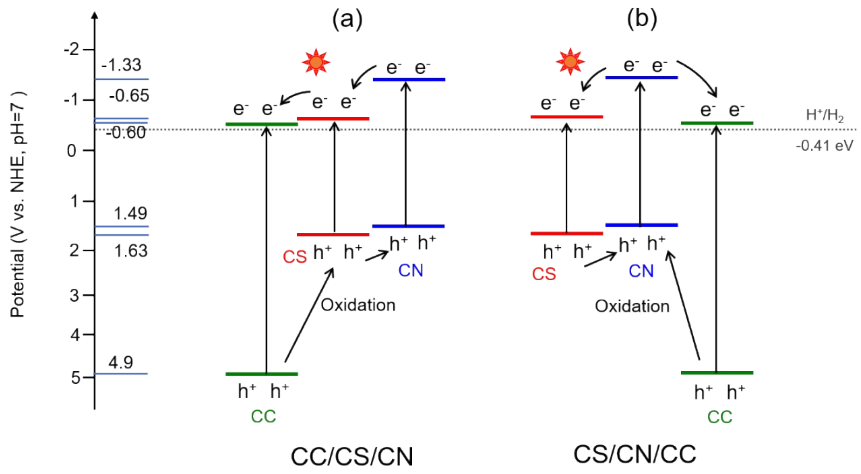

Fig. S8 Possible charge transfer routes of two photoctalysts. (a) CC/CS/CN; (b) CS/CN/CC.

In our study, CC in-situ generated to form CN/CC/CS composite, so the exact same CC could not be synthesized independently. We combine the band configuration of CC in the previous literatures [3] with the results of Fig. 4a-c to obtain the band configuration of different composites in Fig. S8. We assume that CC doesn't exist between CN and CS, then it can only exist on the surface of CN or CS, and thus forming CC/CS/CN or CC/CN/CS composites. The possible charge transfer routes of these two composites are shown in Fig. S8. For CC/CS/CN, all the photogenerated electrons will accumulate on the surface of CC (Fig. S8a). For CC/CN/CS, photogenerated electrons will partially accumulate on the surface of CC and CS (Fig. S8b). Since CC is a wide bandgap semiconductor that cannot absorb visible light, the visible-light-driven hydrogen production performance of CC/CS/CN or CC/CN/CS should not be high, which is not comparable with that of CN/CC/CS (Fig. 5a-b). Undoubtedly, CC exists between CN and CS, and thus forming CN/CC/CS.

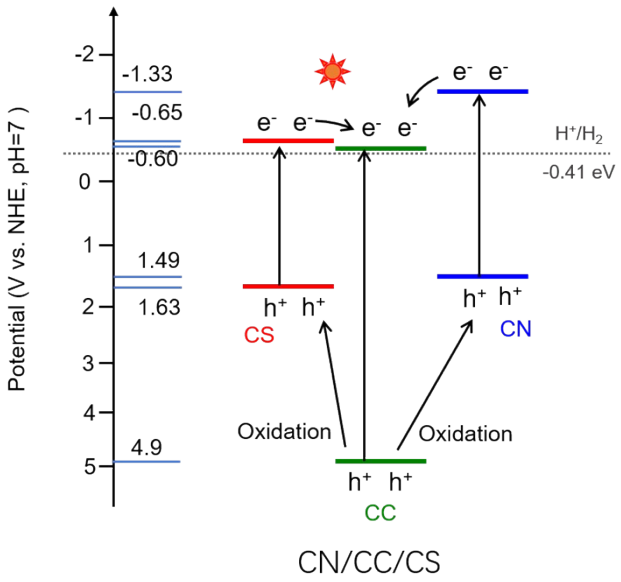

Fig. S9 A dual type II mechanism for CN/CC/CS.

The staggered gap of CN/CC/CS might present two different processes of photoinduced charge carriers transfer. One is the ASS Z-scheme heterojunction in the manuscript (Fig. 4d), and the other is a dual type II heterojunction (Fig. S9). For an ASS Z-scheme mechanism (Fig. 4d and Fig. 6b), electrons in the CB of CS directly recombine with holes in the VB of CN through the in situ-generated intimate contact of CC, while those in the CB of CN and holes in the VB of CS still reside independently on their own CB and VB, and thus showing a high visible-light-driven H_2 production rate (Fig. 5a-b). For a dual type II mechanism (Fig. S9), electrons in the CBs of CN and CS transfer to the CB of CC, meanwhile holes accumulate in the VBs of CN and CS. Due to the wide band gap of CC, the visible-light-driven H_2 production rate of CN/CC/CS with a dual type II mechanism should be much lower than that of CN/CC/CS with an ASS Z-scheme mechanism. Therefore, the as-synthesized CN/CC/CS shows an ASS Z-scheme mechanism rather than a dual type II mechanism.

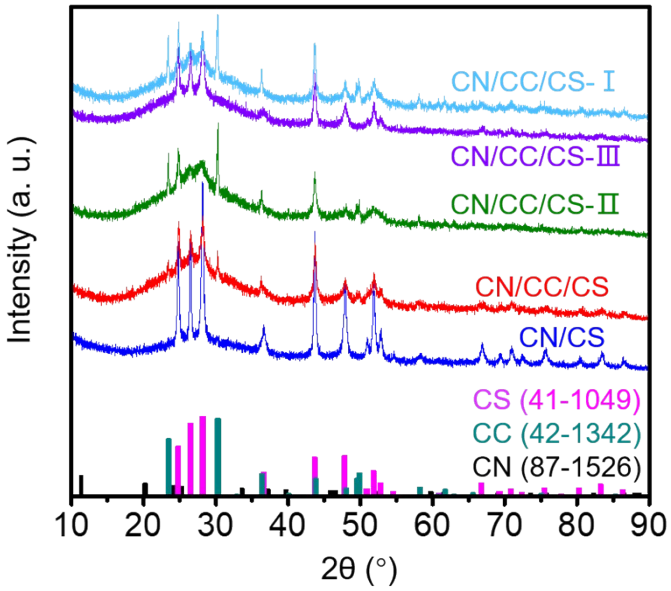

Fig. S10 XRD pattern of various samples. CN/CS, CN/CC/CS, CN/CC/CS-I, CN/CC/CS-II, and CN/CC/CS-III are referred to as 1#, 2#, 3#, 4#, and 5#, respectively.

Table S1 The comparation of other ASS Z-scheme systems for H_2 production.

Photocatalyst	Conductor	Synthetic method	H_2 prodution rate ($\mu mol\ h^{-1}\ g^{-1}$)	ref.
$AgCl/Ag/CaTiO_3$	Ag	Hydrothermal-chemical co-deposition	226.53	4
RP/BP/Co-MOF	Co-MOF	Wet chemistry	140	5
$g\text{-}C_3N_4/rGO/FeOOH$	rGO	Hydrothermal	869.8	6
$Cd_{0.8}Zn_{0.2}S/Au/C_3N_4$	Au	Photochemical deposition	123.21	7
$CNNS/TiN/TiO_{2-x}$	TiN	In situ reduction	1230	8
$CdS/QDs/ZnIn_2S_4$	MoS_2	Hydrothermal	2107.5	9
$g\text{-}C_3N_4/CdCO_3/CdS$	**$CdCO_3$**	**Hydrothermal**	**3521**	**This work**

References

1. Y. Tachibana, L. Vayssieres and J. R. Durrant, *Nat. Photonics*, 2012, **6**, 511-518.
2. H. Li, W. Tu, Y. Zhou and Z. Zou, *Adv. Sci.*, 2016, **3**, 1500389.
3. D. Vidyasagar, S. G. Ghugal, A. Kulkarni, A. G. Shende, S. S. Umare and R. Sasikala, *New J. Chem.,* 2018, **42**, 6322-6331
4. Z. Jiang, J. Pan, B. Wang and C. Li, *Appl. Surf. Sci.*, 2018, **436**, 519-526.
5. L. Hu, J. Xu, S. Zhao, X. Li, L. Li and L. Ran, *Catal. Lett.*, 2021, **151**, 2658-2672.
6. N. Arif, Z.-X. Wang, Y.-T. Wang, Y.-C. **Dou**, K. Li, S.-Q. Liu and F.-T. Liu, *CrystEngComm*, 2021, **23**, 1991-1998.
7. H. Zhao, X. Ding, B. Zhang, Y. Li and C. Wang, *Sci. Bull.*, 2017, **62**, 602-609.
8. D. Yuan, Y. Jiao, Z. Li, X. Chen, J. Ding, W. L. Dai, H. Wan and G. Guan, *Adv. Mater. Interfaces*, 2021, **8,** 2100695.
9. W. Chen, R.-Q. Yan, J.-Q. Zhu, G.-B. Huang and Z. Chen, *Appl. Surf. Sci.*, 2020, **504,** 144406.